

## Durham Research Online

---

### Deposited in DRO:

12 January 2015

### Version of attached file:

Accepted Version

### Peer-review status of attached file:

Peer-reviewed

### Citation for published item:

Bezard, R. and Schaefer, B.F. and Turner, S. and Davidson, J.P. and Selby, D. (2015) 'Lower crustal assimilation in oceanic arcs : insights from an osmium isotopic study of the Lesser Antilles.', *Geochimica et cosmochimica acta.*, 150 . pp. 330-344.

### Further information on publisher's website:

<http://dx.doi.org/10.1016/j.gca.2014.11.009>

### Publisher's copyright statement:

NOTICE: this is the author's version of a work that was accepted for publication in *Geochimica et Cosmochimica Acta*. Changes resulting from the publishing process, such as peer review, editing, corrections, structural formatting, and other quality control mechanisms may not be reflected in this document. Changes may have been made to this work since it was submitted for publication. A definitive version was subsequently published in *Geochimica et Cosmochimica Acta*, 150, 1 February 2015, 10.1016/j.gca.2014.11.009.

### Additional information:

## Use policy

---

The full-text may be used and/or reproduced, and given to third parties in any format or medium, without prior permission or charge, for personal research or study, educational, or not-for-profit purposes provided that:

- a full bibliographic reference is made to the original source
- a [link](#) is made to the metadata record in DRO
- the full-text is not changed in any way

The full-text must not be sold in any format or medium without the formal permission of the copyright holders.

Please consult the [full DRO policy](#) for further details.

1 **Lower crustal assimilation in oceanic arcs: insights**  
2 **from an osmium isotopic study of the Lesser Antilles**

3 **Rachel Bezard<sup>1,2\*</sup>, Bruce F. Schaefer<sup>2</sup>, Simon Turner<sup>2</sup>, Jon P. Davidson<sup>1</sup> and David**  
4 **Selby<sup>1</sup>**

5 <sup>1</sup> *Durham Geochemistry Centre, Department of Earth Sciences, Durham University,*  
6 *South Road, Durham DH1 3LE, UK*

7 <sup>2</sup> *Department of Earth and Planetary Sciences, Macquarie University, University*  
8 *Avenue, Macquarie Park NSW 2113, Australia*

9 *\*Corresponding author. Now at Institut für Planetologie, Westfälische Wilhelms-*  
10 *Universität Münster, Wilhelm-Klemm-Str. 10, 48149 Münster. Germany; E-mail address:*  
11 *bezard@uni-muenster.de; Tel.: +49 251 83 33492; Fax: +49 251 83 36301.*

12

13 **Abstract**

14 We present whole rock  $^{187}\text{Os}/^{188}\text{Os}$  data for the most mafic lavas along the Lesser  
15 Antilles arc (MgO = 5-17 wt. %) and for the subducting basalt and sediments.  $^{187}\text{Os}/^{188}\text{Os}$   
16 ratios vary from 0.127-0.202 in the arc lavas. Inverse correlations between  $^{187}\text{Os}/^{188}\text{Os}$   
17 and Os concentrations and between  $^{187}\text{Os}/^{188}\text{Os}$  and indices of differentiation such as  
18 MgO suggests that assimilation, rather than source variation, is responsible for the range  
19 of Os isotopic variation observed.  $^{87}\text{Sr}/^{86}\text{Sr}$ , La/Sm and Sr/Th are also modified by  
20 assimilation since they all correlate with  $^{187}\text{Os}/^{188}\text{Os}$ . The assimilant is inferred to have a  
21 MORB-like  $^{87}\text{Sr}/^{86}\text{Sr}$  with high Sr (>700 ppm), low light on middle and heavy rare earth  
22 elements (L/M-HREE; La/Sm ~2.5) and  $^{187}\text{Os}/^{188}\text{Os} > 0.2$ . Such compositional features  
23 are likely to correspond to a plagioclase-rich early-arc cumulate. Given that assimilation  
24 affects lavas that were last stored at more than 5 kbar, assimilation must occur in the  
25 middle-lower crust.

26 Only a high MgO picrite from Grenada escaped obvious assimilation (MgO =  
27 17% wt. %) and could reflect mantle source composition. It has a very radiogenic  
28  $^{87}\text{Sr}/^{86}\text{Sr}$  (0.705) but a  $^{187}\text{Os}/^{188}\text{Os}$  ratio that overlaps the mantle range (0.127).  
29  $^{187}\text{Os}/^{188}\text{Os}$  and  $^{87}\text{Sr}/^{88}\text{Sr}$  ratios of the sediments and an altered basalt from the subducting  
30 slab vary from 0.18-3.52 and 0.708-0.714. We therefore suggest that, unlike Sr, no Os  
31 from the slab was transferred to the parental magmas. Os may be either retained in the  
32 mantle wedge or even returned to the deep mantle in the subducting slab.

33 **1. INTRODUCTION**

34 Understanding the behaviour of siderophile elements such as Os in subduction  
35 zones is important for both scientific and economic reasons. Whether Os stays in the  
36 subducting slab, is transferred to residual phases of the upper mantle, or is recycled back  
37 to the crust via the magma needs to be constrained in order to (1) better estimate the  
38 crust-mantle fluxes of siderophile elements throughout Earth evolution; (2) constrain  
39 their application as a powerful isotope tracer to understand subduction processes; and (3)  
40 understand the formation of precious metal ore-bodies.

41 In this context, the origin of radiogenic  $^{187}\text{Os}/^{188}\text{Os}$  ratios within arc lavas,  
42 compared to the depleted upper mantle (DMM), has been debated for more than a decade  
43 (Borg et al., 2000; Alves et al., 2002; Chesley et al., 2002; Righter et al., 2002). While the  
44 enrichment in radiogenic Os could be due to contamination of the mantle wedge by slab  
45 derived fluids/melts (e.g. Borg et al., 2000; Alves et al., 2002), it could also be caused by  
46 assimilation of arc crust during the magmatic ascent (Righter et al., 2002), or both  
47 (Suzuki et al., 2011). Arguments for crustal assimilation include (1) a negative  
48 correlation between  $^{187}\text{Os}/^{188}\text{Os}$  and Os that is observed in most arcs lavas (Chesley et al.,  
49 2002; Righter et al., 2002); (2) the very low Re concentrations in primitive arc lavas  
50 coupled with the results of experimental studies predicting that slab derived-fluids  
51 capable of carrying Os would carry several order of magnitude more Re than Os (Righter  
52 et al., 2002; Xiong and Wood, 1999; 2000). Since both Re and Os were shown to be  
53 similarly volatile (Finnegan et al., 1990), the absence of high Re concentrations in  
54 primitive lavas suggests that Re from the slab is not efficiently transported into primitive  
55 magmas, in which case Os is very unlikely to be transported too; and (3) the very

56 unradiogenic  $^{187}\text{Os}/^{188}\text{Os}$  of some mantle xenoliths from the Japan and Izu Bonin arcs  
57 (Parkinson et al., 1998; Senda et al., 2007) which suggest the absence of enrichment in  
58 radiogenic Os of the mantle wedge. On the other hand, a slab origin for radiogenic Os in  
59 arc lavas is supported by (1) the radiogenic signature of some mantle xenoliths from the  
60 Cascades, Japan, New Ireland and Kamchatka arcs (Brandon et al., 1996; McInnes et al.,  
61 1999; Widom et al., 2003); (2) the trend to more radiogenic  $^{187}\text{Os}/^{188}\text{Os}$  with decreasing  
62 Cr# and increasing  $\text{Fe}^{3+}$  in Cr-spinels from the Izu Bonin arc which suggests an increase  
63 in mobility of slab derived Os during an arc lifetime due to a progressive change in  
64 oxidation state of the mantle (Suzuki et al., 2011); and (3) the existence, in high-pressure  
65 melange zones, of ‘hybrid’ rocks between crustal and mantle materials which display  
66 similar inverse correlation between Os and  $^{187}\text{Os}/^{188}\text{Os}$  to that observed in most arc lavas  
67 (Penniston-Dorland et al., 2012; 2014)

68         The Lesser Antilles arc (Fig. 1) is an excellent natural laboratory to investigate the  
69 mobility of Os in subduction zones since: (1) very primitive lavas such as picrites with  
70  $\text{MgO} = 17.4$  (wt. %) can be sampled; (2) very radiogenic Os should be subducted in the  
71 southern part of the subduction zone where the slab contains organic-rich sediments  
72 (black shales); and (3) the arc lavas and the subducting slab sediment/basalts are both  
73 very well constrained in terms of major, trace elements and radiogenic isotopes.  
74 Accordingly, we have analysed the most mafic and well constrained lavas from along the  
75 arc, as well as representative sediments and altered basalt from the subducting slab.

76

## 77 **2. SAMPLES AND ANALYTICAL METHODS**

### 78 **2.1 Samples**

79           We selected the most mafic lava samples (MgO=5-17 wt. %) available from 7  
80 different islands along the Lesser Antilles arc (n=8), as well as an altered basalt (n=1;  
81 DSDP site 543), an organic-poor sediment (n=1; DSDP site 543) and organic-rich  
82 sediments including black shales (n=11; Unit 3-5 DSDP site 144) from the subducting  
83 American Plate (Tables 1 and 2).

84           The sediments were selected to characterize a key north-south difference in the  
85 nature of the subducting sediments, likely to be reflected in their Os isotopic signature.  
86 The nature and composition of the sediments present at the front of the arc was  
87 investigated by Hayes et al. (1972), Pudsey and Reading (1982) and Biju-Duval et al.  
88 (1984; 1985) using cored sediments from the DSDP site 543 for the northern sequences  
89 and DSDP site 144 and Barbados sediments for the southern sequences. These studies  
90 showed that the northern subducting pile (north of Martinique) was dominated by clays  
91 and radiolarites while the southern subducting pile (Martinique and southward) was  
92 mainly composed of clay and carbonate with the occurrence of significant amounts of  
93 organics (up to 30%), biogenic silica (up to 30%) and detrital quartz (up to 40%) in some  
94 units. In terms of Os isotopes, the most important difference between the northern and the  
95 southern sequences is the presence of (Late Cretaceous) organic-rich layers at the base of  
96 the southern sedimentary pile (the absence of such organic-rich units in the north is due  
97 to the younger age of the subducting plate, as supported by the magnetic map of the  
98 Atlantic Ocean floor at the front of the arc). This is because organic-rich sediments  
99 typically concentrate Re during deposition and are expected to present higher  $^{187}\text{Os}/^{188}\text{Os}$   
100 than organic-poor sediments, due to Re decay. The presence of more radiogenic Os in the  
101 southern subducting pile could in turn be reflected in the lava compositions. Therefore,

102 analysing both organic-rich and organic-poor sediments is important to understand if, as  
103 predicted, they have different isotopic composition.

104         The organic-poor sediment analysed consists of early Miocene clay with minor  
105 ash (Biju-Duval et al., 1984). The organic-bearing sediments selected record  
106 sedimentation preceding (Unit-5-4; up to 5% organics; Late-Aptian to lower  
107 Cenomanian; Carpentier et al., 2008) and contemporaneous (Unit-3; up to 30% organics;  
108 Lower Turonian to Santonian) with the oceanic anoxic event 2 (OAE2; 93.5 My e.g.  
109 Turgeon and Creaser, 2008). Samples from Unit 5 consist of quartzose carbonaceous clay  
110 or mudstone while Unit 4 sample is marl. Finally samples from Unit 3 are zeolitic  
111 calcareous carbonaceous black shale (Hayes et al., 1972).

112         By selecting the most mafic lavas, we attempted to minimise the effects of  
113 assimilation of continent-derived sediment present in the arc crust. Such sediment is  
114 responsible for the extreme isotopic compositions observed in the central-southern parts  
115 of the arc (e.g. Davidson, 1987; Bezard et al., 2014). All lavas (Fig. 2) and sediments  
116 have previously been analysed for major, trace elements and Sr-Nd isotopes (Davidson,  
117 1984; Davidson, 1986; Heat et al., 1998; Van Soest, 2000; Dufrane et al., 2009; see Table  
118 2). The most primitive lava sampled, which is also the most primitive lava in the arc, is  
119 an olivine and plagioclase phyric picrite from Grenada (LAG4) with both high MgO  
120 (17.4 wt. %) and Mg# (77.4) (Van Soest, 2000). It belongs to the abundant M-series suite  
121 of picrites found on the island. Previous studies on M-series picrites with MgO as high as  
122 15.5 wt. % suggested that these were primary mantle melts by precluding olivine  
123 phenocrysts accumulation, or incorporation of mantle xenocrysts, as the cause of their  
124 high MgO. LAG 4 olivine crystals have similar Mg# in cores (90-82) and rims (89-82)

125 which does not support a xenocrystic origin of the crystals. Furthermore, the  $D_{Ni}$   
126 calculated from the picrite MgO ( $D_{Ni} = 6.27$ ; using Hart and Davis (1978) equation) is  
127 similar to the  $D_{Ni}$  calculated using the whole rock and the mean olivine Ni concentrations  
128 ( $D_{Ni} = 6.67$ ; using probe data from Van Soest (2000)). This suggest that the Ni content in  
129 the olivine crystals is consistent with that expected from crystals growing in a magma  
130 with an MgO similar to that of LAG4 and that no significant olivine accumulation or  
131 mantle xenocryst incorporation should have occurred. Out of the samples selected, it  
132 displays the highest Light on Middle Rare Earth Element ratio (L/M-HREE), the lowest  
133 Sr/Th and the most radiogenic Sr isotopic composition (Sr/Th = 123;  $^{87}Sr/^{86}Sr = 0.7051$ ;  
134 Fig. 2). Such features characterise all Grenada primitive lavas when compared to basaltic  
135 lavas from other islands of the arc (Macdonald et al., 2000). St Vincent contains very  
136 mafic lavas (MgO = 12.6 wt. %) with phenocryst assemblages dominated by olivine  
137 (traces of Cpx and Ti-magnetite). A less primitive basalt from the same island (MgO =  
138 5.12 wt. %) mainly presenting plagioclase, olivine and clinopyroxene phenocrysts was  
139 also analysed. The most primitive lavas from the remaining islands (Saba, Redonda,  
140 Guadeloupe, Martinique and St Lucia) have MgO contents that range from 5.1 to 8.7 (wt.  
141 %). Their phenocryst assemblage comprise olivine crystals and variable amount of  
142 clinopyroxene and plagioclase. All of the lavas selected are 1 Ma old or younger with the  
143 exception of the St Lucia lava flow which is dated at 11 Ma (Table 1).

## 144 **2.2. Analytical methods**

145 All samples, except the organic-rich sediments, were analysed for Os and  
146  $^{187}Os/^{188}Os$  at the Geochemical Analysis Unit (GAU) at Macquarie University. The  
147 organic-rich sediments were analysed for Re, Os and isotope compositions ( $^{187}Re/^{188}Os$ ;



148  $^{187}\text{Os}/^{188}\text{Os}$ ) at the TOTAL Laboratory for Source Rock Geochronology and  
149 Geochemistry which is part of the Durham Geochemistry Centre (DGC) at Durham  
150 University.

151 At Macquarie, whole rock powders (2-5g) (produced in agate ball mills) were  
152 spiked for Os and digested using large carius tubes (60 cm<sup>3</sup>) in inverse *aqua-regia* using  
153 double Teflon distilled reagents at 220°C for 3 days. Given the young age of the samples,  
154 no age correction on the  $^{187}\text{Os}/^{188}\text{Os}$  ratio was necessary and Re was not analysed. Os was  
155 separated by solvent extraction following the method of Cohen and Waters (1996) and  
156 was analysed by negative thermal ion mass spectrometry (N-TIMS) on the electron  
157 multiplier (SEM) of the Thermo-Finnigan Triton mass spectrometer at Macquarie  
158 University in dynamic mode. All data were blank corrected using the total procedural  
159 blank (TPB) processed with the samples analysed. TPB was 6.30 pg Os with an  
160  $^{187}\text{Os}/^{188}\text{Os}$  ratio of 0.1821 (n=1). This corresponds to corrections of 0-12% except for the  
161 two lavas with the lowest abundances where these corrections amounted to 21 and 25%.  
162 During the analytical session, instrument performance was monitored by analysis of Os  
163 in-house solution standard JMC-2.  $^{187}\text{Os}/^{188}\text{Os}$  for 5 ng loads in dynamic collection mode  
164 was  $0.18311 \pm 0.00016$  (2SD; n=4) which is in good agreement with the long term  
165 running means of 5ng JMC-2 in dynamic mode of  $0.18294 \pm 0.00070$  (2SD; n=17 since  
166 2006). The performance of the instrument when running small loads similar to the lavas  
167 was verified by the analysis of ~1.7ng loads of WPR-1 (0.1g digested). The average  
168  $^{187}\text{Os}/^{188}\text{Os}$  ratio of the WPR-1 international rock standard was  $0.1451 \pm 0.0013$  (2SD;  
169 n=4) with concentrations of  $17.19 \text{ ppb} \pm 0.71$  (2SD; n=4) which is in good agreement

170 with the accepted values (Cohen and Waters, 1996;  $^{187}\text{Os}/^{188}\text{Os} = 0.14543 \pm 0.00018$   
171 (2SD) and  $\text{Os} = 16.06 \text{ ppb} \pm 0.8$  (2SD)).

172 At Durham, the organic-rich whole rock powders were also analysed by isotope-  
173 dilution negative thermal ionization mass spectrometry. Prior to being powdered, all the  
174 samples were cleaned to remove any minor drill marks using a diamond polish cloth with  
175 no polishing agent, except water. Samples were pre crushed without metal contact and  
176 then powdered in a Zr dish. A dried sample weight of  $\geq 30 \text{ g}$  was powdered in order to  
177 homogenise the Re and Os within the sample (Kendall et al., 2009). The Re-Os isotopic  
178 analysis was conducted using Carius tube digestion in a 0.25 g/g  $\text{CrO}_3$  4N  $\text{H}_2\text{SO}_4$  reagent  
179 at  $220^\circ\text{C}$  for 48hrs with the Re and Os isolated from the acid medium using solvent  
180 extraction, micro-distillation and anion chromatography methodology (Selby and  
181 Creaser, 2003). This method preferentially liberates hydrogenous Re-Os (Selby and  
182 Creaser, 2003; Kendall et al. 2009 and references therein). In brief,  $\sim 0.5 \text{ g}$  of sample  
183 powder was loaded in a Carius tube with a known amount of mixed tracer solution.  $^{190}\text{Os}$   
184 +  $^{185}\text{Re}$ , with 8 ml of  $\text{CrO}_3$ - $\text{H}_2\text{SO}_4$  solution. The sealed Carius tubes were then placed in  
185 an oven at  $220^\circ\text{C}$  for 48 hrs. Osmium was isolated and purified using solvent extraction  
186 ( $\text{CHCl}_3$ ) and microdistillation methods. Anion chromatography was used to purify the Re  
187 from 1 ml of the  $\text{CrO}_3$ - $\text{H}_2\text{SO}_4$  solution (Selby and Creaser, 2003). The purified Re and Os  
188 fractions were loaded onto Ni and Pt filaments, respectively (Selby and Creaser, 2003)  
189 with the addition of  $\sim 0.5 \mu\text{l}$   $\text{BaNO}_3$  and  $\text{BaOH}$  activator solutions, respectively. Isotope  
190 compositions were measured using N-TIMS (Creaser et al., 1991; Volkening et al., 1991)  
191 via faraday cups for Re and electron multiplier in peak hopping mode for Os. All samples  
192 were analysed as one batch. For this batch the total procedural blank for Re and Os

193 during this study is  $13.3 \pm 1.8$  pg and  $0.32 \pm 0.17$  pg, respectively, with  $^{187}\text{Os}/^{188}\text{Os}$  value  
194 of  $0.19 \pm 0.05$ . Uncertainties for  $^{187}\text{Re}/^{188}\text{Os}$  and  $^{187}\text{Os}/^{188}\text{Os}$  are determined through full  
195 propagation of uncertainties in Re and Os mass spectrometer measurements, blank  
196 abundances and isotopic compositions, spike calibrations and reproducibility of standard  
197 Re and Os isotopic values. In-house standard solutions (DROsS and Re Std) are  $0.16094$   
198  $\pm 0.00030$  and  $0.5980 \pm 0.0032$  (2 S.D.), which are consistent within uncertainty to those  
199 published by Nowell et al. (2008). Additionally at Durham, sample Re-Os data  
200 reproducibility is monitored using the USGS rock reference material SDO-1 (Devonian  
201 Ohio Shale). Average (2 S.D.) Re-Os data for SDO-1 are:  $75.5$  ppb  $\pm 11.3$  Re, and  $626.1$   
202 ppt  $\pm 101.8$  Os, and  $1166.0 \pm 88.1$   $^{187}\text{Re}/^{188}\text{Os}$  and  $7.831 \pm 0.568$   $^{187}\text{Os}/^{188}\text{Os}$  (Du Vivier  
203 et al., 2014).

### 204 3. RESULTS

205 All  $^{187}\text{Os}/^{188}\text{Os}$  and Os concentrations as well as  $^{187}\text{Re}/^{188}\text{Os}$  and Re for the  
206 organic-rich sediments are presented in Table 1 and corresponding lithophile element  
207 concentrations and isotopic ratios from the literature are presented in Table 2. All lavas  
208 apart from the most mafic sample, (Grenada picrite; MgO = 17 wt. %), have more  
209 radiogenic  $^{187}\text{Os}/^{188}\text{Os}$  than the depleted mantle range (DMM;  $^{187}\text{Os}/^{188}\text{Os} = 0.1238 \pm$   
210  $0.0042$ ; Rudnick and Walker (2009)) and variable  $^{187}\text{Os}/^{188}\text{Os}$  ratios and Os  
211 concentrations ranging between 0.127-0.202 and 0.005-0.362 ppb respectively (Fig. 3).  
212 The  $^{187}\text{Os}/^{188}\text{Os}$  ratio of the altered basalt is 0.466 and this sample has a very low Os  
213 abundance (0.0095 ppb). The organic-poor claystone from DSDP site 543 is enriched in  
214 Os (11.15 ppb) and possesses moderately radiogenic  $^{187}\text{Os}/^{188}\text{Os}$  (0.185). The most  
215 organic-rich sedimentary units from DSDP 144 (Unit 3) have highly radiogenic

216  $^{187}\text{Os}/^{188}\text{Os}$  (1.33-3.25) and moderate Os concentrations (0.10-0.94 ppb), while the older  
217 units (4 and 5), which are characterized by lower organic matter content, have moderately  
218 radiogenic  $^{187}\text{Os}/^{188}\text{Os}$  (0.32-0.72) and variable Os concentrations from 0.09 to 34.48  
219 ppb. (Fig. 3). The abundances of Os in all sediments analysed is above that of average  
220 continental crust (<50 ppt; Peuker-Ehrenbrink and Ravizza, 2000). The isotopic  
221 variations observed between Unit 3 and Units 4 and 5 are also observed in the calculated  
222 initial  $^{187}\text{Os}/^{188}\text{Os}$  ratio (using sediment ages from Hayes et al. (1972) and Carpentier et  
223 al. (2008); Table 1) which indicates that part of the isotopic variations observed in site  
224 144 sediment are not due to variations in Re content. Given that the analytical method  
225 used for these sedimentary units preferentially liberates hydrogenous Re and Os and not  
226 detrital associated Re-Os, the variations of the initial isotopic ratios need to be inherited  
227 from sea water compositional variations during sediment deposition.

## 228 **4. DISCUSSION**

### 229 **4.1 Crustal assimilation control on $^{187}\text{Os}/^{188}\text{Os}$**

230 In the Lesser Antilles arc, all studies addressing the quantification of the  
231 subducting slab derived components in the magma source, using the isotopic (Sr, Nd, Pb,  
232 Hf, U-series) and trace element composition of the lavas, suggested either a similar (e.g.  
233 Davidson and Wilson (2011); Dufrane et al. (2009)) or increasing amount of sediment in  
234 the mantle source along the arc (e.g. Carpentier et al., 2008). Therefore, if transfer of  
235 slab-derived Os into the mantle wedge was to be reflected in the isotopic variations  
236 observed in the lavas, a north-south trend to more radiogenic  $^{187}\text{Os}/^{188}\text{Os}$  in the lavas  
237 should be observed. This is because the dominantly organic-poor sediment sequences

238 subducted in the north have markedly less radiogenic  $^{187}\text{Os}/^{188}\text{Os}$  than the sequences  
239 subducted in the south which comprise organic-rich sediments. However, no such  
240 geographic variation is observed. Indeed the least radiogenic compositions are observed  
241 in lavas from the south of the arc, in Grenada and St Vincent. These observations argue  
242 against the direct control of lava isotopic variations by slab-derived Os. Instead, the  
243 samples form inverse correlations between  $^{187}\text{Os}/^{188}\text{Os}$  and both Os (0.005-0.36) (Fig. 4a)  
244 and MgO (Fig. 4b) with compositions of the southern lavas plotting on a steeper trend  
245 than the northern islands (from Martinique northward). These negative correlations  
246 between an index of differentiation and  $^{187}\text{Os}/^{188}\text{Os}$  cannot easily be produced in the  
247 mantle source since it would either need to be explained by (1) a mantle source with  
248 homogeneous MgO, affected by a process able to enrich it in  $^{187}\text{Os}$  and additionally  
249 control the future extent of magmatic differentiation; or (2) a heterogeneous source  
250 characterized by coupled variations in MgO and  $^{187}\text{Os}/^{188}\text{Os}$  (e.g. in sources with a  
251 different mineralogy due to metasomatism, such as a peridotitic mantle comprising  
252 pyroxenites) that would be transmitted to the magma and conserved until eruption. Both  
253 scenarios seem very unlikely since the degree of lava differentiation is known to be  
254 influenced by the structure and thickness of the crust, both thought to be heterogeneous  
255 along the arc (e.g. Boynton et al., 1979). Therefore, the  $^{187}\text{Os}/^{188}\text{Os}$  variations in the  
256 Lesser Antilles arc lavas is more likely accounted for by a process, or processes, which  
257 postdate mantle melting. Since both trends formed by lavas from the southern and  
258 northern islands back project toward the composition of the Grenada picrite (Fig. 4), they  
259 could be explained by evolution from a common parental magma. The differences in  
260 subsequent magmatic evolution may reflect either different phases fractionated during

261 assimilation with different partitioning for MgO and Os, different rates of assimilation or  
262 slightly different  $^{187}\text{Os}/^{188}\text{Os}$  ratios of the putative assimilants.

263 Control of the osmium isotopic composition by assimilation rather than by slab  
264 contributions is emphasized when the  $^{187}\text{Os}/^{188}\text{Os}$  ratios of both lavas and sediments are  
265 plotted against Sr isotope ratios (Fig. 5a). Once again, a negative correlation is observed  
266 for the lavas with a decrease in  $^{87}\text{Sr}/^{86}\text{Sr}$  with increasing  $^{187}\text{Os}/^{188}\text{Os}$ . This negative  
267 correlation precludes the simple mixing of sediment-derived Os in the lavas sources since  
268 the sediments display both radiogenic Sr and Os and a mixing line between the mantle  
269 and the sediments would therefore have a positive slope which is the opposite of that  
270 observed (Fig. 5a). Although the altered basalt from the slab has a lower Sr isotopic  
271 composition than the sediment, mixing of fluids derived from this component with the  
272 mantle wedge would also result in a positive trend.

273 A source process capable of increasing slab-derived Os while decreasing slab  
274 derived Sr in the mantle is inconsistent with the decrease in Os concentrations observed  
275 with increasing  $^{187}\text{Os}/^{188}\text{Os}$  (Fig. 4a). So too, stabilisation of an Os-bearing phase in the  
276 mantle wedge due to fluid fluxing from the slab (Borg et al., 2000) is inconsistent with  
277 the covariant decrease in both MgO and Os (Fig. 4a,b).

278 An increase in slab derived Os mobility in response to increasing the oxidation  
279 state of the mantle through time (Suzuki et al., 2011) is inconsistent with the decrease in  
280  $^{87}\text{Sr}/^{86}\text{Sr}$  observed with the increasing  $^{187}\text{Os}/^{188}\text{Os}$  (Fig. 5a). Indeed slab derived Sr  
281 mobility is very unlikely to be sensitive to variation in oxygen fugacity given that, unlike  
282 Os, Sr displays only one valence state (bivalent) under normal geological conditions.

283 Instead, the contents of slab-derived Sr in the mantle are likely to be controlled by the  
284 extent of slab-derived fluid fluxing through the wedge, the latter fluid being also  
285 responsible for the increase in mantle oxygen fugacity through time (Brandon and  
286 Draper, 1996). Therefore, an increase rather than a decrease in slab derived Sr with  
287 increasing mantle oxygen fugacity would be expected. For example, such positive  
288 correlation between Sr concentration and oxygen fugacity was observed in melt  
289 inclusions from primitive lavas in the Cascades (Rowe et al., 2009). Furthermore,  
290 because the increase in  $^{187}\text{Os}/^{188}\text{Os}$  ratios correlates inversely with MgO, any postulated  
291 increase in oxygen fugacity of the mantle would need to have a tight control on the future  
292 degree of differentiation of the magma, which seems very unlikely.

293 Finally, a complex case occurring at the slab-mantle interface and involving (1) a  
294 mechanical mixing of ultramafic and mafic material from the subducting slab around  
295 blocks of subducted basalts and (2) the metasomatism of the resulting hybrid rocks by  
296 sediment-derived fluids, was shown to produce a suite of rocks with similar negative  
297 correlation between Os, MgO and  $^{187}\text{Os}/^{188}\text{Os}$  to that observed in the Lesser Antilles  
298 lavas (Penniston-Dorland et al., 2012; 2014). A negative correlation between  $^{87}\text{Sr}/^{86}\text{Sr}$   
299 and  $^{187}\text{Os}/^{188}\text{Os}$  in these hybrid rocks would also be predicted. It has been suggested that,  
300 if these rocks from the slab-mantle interface ascended within diapirs to the base of the arc  
301 lithosphere (e.f. Marschall and Schumacher, 2012), these heterogeneities could be  
302 directly reflected in the arc lavas (Penniston-Dorland et al., 2012; 2014). However, as  
303 mentioned in the previous section, if the correlation observed in the lava compositions  
304 resulted from a direct reflection of these source heterogeneities, then no, or similar  
305 amounts of differentiation would need to have occurred for all lavas analysed, which

306 seems unlikely. Furthermore, rocks in the melange having  $^{187}\text{Os}/^{186}\text{Os}$  out of the mantle  
307 range are dominantly made of altered basalt and should therefore have high  $\delta^{18}\text{O}$   
308 signatures which would be transferred to the related magma. This scenario is inconsistent  
309 with the mantle like  $\delta^{18}\text{O}$  of the olivine and pyroxene crystals analysed in the Lesser  
310 Antilles lavas with the highest  $^{187}\text{Os}/^{188}\text{Os}$  ratios. Therefore, although source  
311 contamination cannot be completely ruled out, it is considered highly unlikely, and the  
312 trends defined by the lavas seem more plausibly explained by a process occurring after  
313 melting in the source, .i.e. crustal assimilation.

#### 314 **4.2 Source $^{187}\text{Os}/^{188}\text{Os}$**

315         Since crustal assimilation appears to have affected lava  $^{187}\text{Os}/^{188}\text{Os}$  during  
316 differentiation in the Lesser Antilles, the only sample suitable for constraining source  
317 characteristics is the sample with the highest MgO and highest Os concentrations, which  
318 is the picrite from Grenada (LAG4). This picrite  $^{187}\text{Os}/^{188}\text{Os}$  (0.1267) plots within the  
319 mantle range ( $\text{DMM} = 0.1238 \pm 0.0042$ ) (Fig. 4a, b) which indicates that assimilation had  
320 no, or very limited (in the case where the ambient mantle lies in the lower hand of the  
321 DMM range), effect on its composition and that it therefore represent the lava with the  
322 closest composition to that of the mantle source region. The apparent absence, or very  
323 limited amount, of radiogenic Os from either the subducting altered basalt or sediments in  
324 the Grenada picrite indicates either that (1) Os from the subducting slab is not, or not  
325 efficiently, transported into the magma source regions or (2) that it was retained in a  
326 residual mantle phase before the primitive Grenada melts were generated.

327         Conversely, the Grenada picrite has very radiogenic  $^{87}\text{Sr}/^{88}\text{Sr}$  (0.70508; Fig 5a)  
328 which indicates that, as expected, Sr was mobilised from the slab into the wedge. As



329 mentioned earlier, the more radiogenic Sr isotopic ratio of the Grenada picrite analysed,  
330 compared to other islands of the arc, is a general feature of Grenada mafic lavas, which  
331 has often been interpreted to reflect a greater contribution of sediment to the mantle  
332 source (Thirlwall et al., 1996). However, we show that Sr isotopes correlate inversely  
333 with Os isotopes which appear to be controlled by assimilation. Therefore, the negative  
334 trend in  $^{87}\text{Sr}/^{86}\text{Sr}$  observed in the Lesser Antilles lavas would need to be accounted for by  
335 the same process. Hence  $^{87}\text{Sr}/^{88}\text{Sr}$  in the Grenada picrite may not be more radiogenic than  
336 primary magmas of the other islands along the arc but instead provide the only true  
337 representative indication of source  $^{87}\text{Sr}/^{86}\text{Sr}$  prior to crustal assimilation. In this case,  
338 estimations of slab contributions to the magma source based on Sr isotopes in mafic lavas  
339 would have historically been misestimated for most islands.

#### 340 **4.3 Characteristics and nature of the assimilant**

##### 341 *4.3.1 Trace element and isotopic characteristics*

342 As described in section 4.1, the lavas show an inverse correlation between  
343  $^{87}\text{Sr}/^{86}\text{Sr}$  and  $^{187}\text{Os}/^{188}\text{Os}$  (Fig. 5a). However, unlike MgO and Os vs.  $^{187}\text{Os}/^{188}\text{Os}$ , where  
344 two trends are observed, no north-south separation of the data exists. Given that isotopic  
345 ratios are not affected by crystal fractionation, we suggest that the same assimilant is  
346 present in both the north and the south of the arc and that the north-south trends observed  
347 on plots of MgO and Os vs.  $^{187}\text{Os}/^{188}\text{Os}$  can be accounted for by different fractionated  
348 assemblages during assimilation (i.e. different bulk partition coefficients). For example,  
349 fractionation of olivine during assimilation will produce a steeper decrease in MgO and  
350 Os compared with clinopyroxene fractionation.

351           Given that  $^{87}\text{Sr}/^{86}\text{Sr}$  decreases down to  $\sim 0.703$ , the assimilant must have  $^{87}\text{Sr}/^{86}\text{Sr}$   
352 close to the DMM (Salters and Stracke, 2004), which precludes any sedimentary origin  
353 and is in agreement with the mantle-like clinopyroxene and olivine  $\delta^{18}\text{O}$  data available  
354 for some of the high  $^{187}\text{Os}/^{188}\text{Os}$  lavas, which are similar to those of Grenada picrites  
355 (Saba:  $\delta^{18}\text{O}_{\text{ol}} = 5.13$  and  $\delta^{18}\text{O}_{\text{cpx}} = 5.74$  for LAS1; Guadeloupe:  $\delta^{18}\text{O}_{\text{ol}} = 5.00\text{-}5.12$  and  
356  $\delta^{18}\text{O}_{\text{cpx}} = 5.51$  for GUAD510; Grenada:  $\delta^{18}\text{O}_{\text{ol}} = 5.18$  for LAG4; Van Soest et al., 2002).  
357 No clear correlation between Pb isotopes and  $^{187}\text{Os}/^{188}\text{Os}$  can be observed and no  
358 correlation between  $^{143}\text{Nd}/^{144}\text{Nd}$  and  $^{187}\text{Os}/^{188}\text{Os}$  exist (not shown). This could either  
359 indicate that the isotopic composition of the assimilant is similar to that of the primitive  
360 magma, or that the concentrations in Pb and Nd in the assimilant are not high enough to  
361 buffer existing source variations between islands.

362           When La/Sm or La/Yb are plotted against  $^{187}\text{Os}/^{188}\text{Os}$  (Fig. 5b), the same negative  
363 correlation observed on plots of MgO and Os vs.  $^{187}\text{Os}/^{188}\text{Os}$  exists. Such correlations  
364 suggest that the REE were affected during assimilation. As with MgO and Os, we  
365 propose that the separation of the samples into two similar trends is due to different  
366 phases being fractionated during assimilation. The decrease in L/M-HREE in itself  
367 (observed in both trends) could therefore reflect the interplay of the progressive  
368 incorporation of a low La/Sm assimilant and of fractional crystallization of minerals that  
369 fractionate L/M-HREE (such as clinopyroxene or amphibole).

370           Finally, Sr/Th seems also affected by crustal assimilation since it correlates  
371 negatively with  $^{187}\text{Os}/^{188}\text{Os}$  (Fig. 5c). The correlation is clearly due to increasing Sr since  
372 Th does not decrease with  $^{187}\text{Os}/^{188}\text{Os}$ . As for  $^{87}\text{Sr}/^{88}\text{Sr}$  vs.  $^{187}\text{Os}/^{188}\text{Os}$ , no distinction  
373 between the north-south sections of the arc can be observed, consistent with a common

374 assimilant composition along the arc. The assimilant must also have very high Sr content  
375 with a minimum Sr/Th of 624 (the highest ratio found in the lavas).

376 In summary, the isotopic and trace element composition of the lavas suggest that  
377 one of the assimilants present in the basement of Lesser Antilles islands (the other being  
378 continent-derived sediment, not discussed here) displays a mantle-like  $^{87}\text{Sr}/^{88}\text{Sr}$  ratio, a  
379  $^{187}\text{Os}/^{188}\text{Os}$  higher than 0.2, a high Sr/Th ( $> 620$ ), and a low La/Sm and La/Yb.  
380 Significantly, thermobarometric estimations performed on St Vincent picrite (STV301)  
381 indicate that it was last stored at depths corresponding to the arc middle-lower crust (Heat  
382 et al., 1998; Pichavant et al., 2007). This would imply that assimilation would need to  
383 have occurred at depths equivalent to or greater than these.

#### 384 *4.3.2 Nature of the assimilant*

385 Recent ( $\sim$  late Cretaceous to Paleogene) altered Mid-Ocean Ridge Basalts  
386 (MORB) or Fore-arc Basalts (FAB; Reagan et al. (2010)) could have a DMM-like  
387  $^{87}\text{Sr}/^{86}\text{Sr}$  with  $^{187}\text{Os}/^{188}\text{Os}$  higher than 0.2 and low L/M-HREE (typically  $<1$ ), but their Sr  
388 concentration is typically far too low (typically  $\leq 90$  ppm) to be able to modify the  
389 primitive magma concentrations. Bulk mafic MORB or FAB cumulates would also be  
390 too depleted in Sr to represent an appropriate assimilant. Instead, we suggest that the  
391 assimilant could be MORB or FAB plagioclase-rich cumulates present in the lower crust.  
392 Given that the Lesser Antilles arc is thought to be built on the Aves ridge (extinct arc)  
393 forearc after a slab rollback that displaced the activity eastward, FAB cumulates are more  
394 likely to be present at the base of the Lesser Antilles arc than MORB cumulates. Such  
395 rocks would likely occur under every island and meet the geochemical requirements of

396 the assimilant described above. They could comprise mafic layers, but the more felsic  
397 sections would be preferentially assimilated by primitive magmas. While the mafic layers  
398 of cumulates tend to concentrate the iridium platinum group element (IPGE) because  
399 these elements are removed from the melt early during differentiation and concentrate in  
400 cumulus phases such as olivine or chromite, plagioclase-rich layers tend to concentrate  
401 more Re (and palladium platinum group elements: PPGE) since it remain longer in the  
402 melt and is more likely to be present as interstitial sulfides. Radiogenic Os, produced by  
403 Re decay, is therefore more likely to be present in such layers. Since the Lesser Antilles  
404 arc started accreting during the Oligocene (Germa et al., 2011), it would be predicted that  
405 the early-arc FAB lavas and cumulates would have a moderately radiogenic  $^{187}\text{Os}/^{188}\text{Os}$ ,  
406 consistent with the signature of the assimilant. The mantle-like Sr isotopic composition of  
407 the cumulate would also be consistent with their production early in the arc existence,  
408 prior to significant fluids fluxing through the mantle.

409 Finally, none of the lavas analysed have a europium positive anomaly, the latter  
410 being expected in the case of assimilation of large amounts of plagioclase. However, all  
411 but one lava (STV301) contain plagioclase phenocrysts which indicate that plagioclase  
412 fractionation may have erased any such positive anomaly. The absence of any Eu  
413 anomaly in the plagioclase-free high-MgO basalt from St Vincent could be explained by  
414 the low amount of assimilation involved in that lava (~ 7%; Fig. 6) or if the assimilated  
415 plagioclase cumulates did not have a significant positive Eu anomaly. A low Eu anomaly  
416 in plagioclase can only occur in highly oxidised magmas. Since the plagioclase cumulates  
417 are likely to have crystallised at the initiation of the subduction zone, their oxygen  
418 fugacity is likely to be similar to that of FAB erupted at the onset of the Mariana

419 subduction, which have been shown to present high oxygen fugacity (QFM +0.4;  
420 Brounce et al., 2013), and are likely to crystallise plagioclase with small Eu anomalies.

#### 421 *4.3.3 Assimilation and fractional crystallisation (AFC) modelling*

422 The AFC equation (DePaolo, 1981) can be used to model the  $^{187}\text{Os}/^{188}\text{Os}$ ,  
423  $^{87}\text{Sr}/^{88}\text{Sr}$ , La/Sm and Sr/Th relationships using reasonable parameters (Figs. 6a, b, c). We  
424 used the Grenada picrite (LAG4) for the initial magma composition, since it plots within  
425 the mantle range in terms of  $^{187}\text{Os}/^{188}\text{Os}$  and its Os concentration (360 ppt Os) is  
426 consistent with that expected with a melt in equilibrium with sulfide-bearing mantle. The  
427 range of Os, Sr, Th, La and Sm bulk partition coefficients (D) (Table 3) were estimated  
428 by dividing the concentration of these elements in the Grenada picrite by their  
429 concentration in the most differentiated samples. Sr, Th, La and Sm bulk D's obtained are  
430 consistent with fractionation of the observed phenocryst assemblages (olivine  $\pm$  pyroxene  
431  $\pm$  plagioclase). The Os bulk partition coefficients used (D = 12-16) are in agreement with  
432 that expected for  $\sim 0.5\%$  of chromian-spinel fractionation (Chesley et al., 2002; Righter et  
433 al., 2002). The  $^{187}\text{Os}/^{188}\text{Os}$  ratio of the assimilant ( $^{187}\text{Os}/^{188}\text{Os} = 0.245$ ) can be easily  
434 produced by radiogenic ingrowth of a DMM composition with an initial ratio of  
435  $^{187}\text{Os}/^{188}\text{Os}$  (0.127). This could occur within the 25 My since magmatism was initiated in  
436 the Lesser Antilles (Germa et al., 2011), even if the initial  $^{187}\text{Re}/^{188}\text{Os}$  is lower than  
437 MORB ( $\sim 600$ ). The Os concentration of the assimilant used in the model (20 ppt) is  
438 consistent with that expected from a plagioclase-rich cumulate grown from the residual  
439 melt of a MORB/FAB primitive magma (with  $\sim 350$ -200 ppt Os; derived from a sulfide-  
440 bearing mantle) after fractionation of important amounts of olivine and spinel. Indeed 20  
441 ppb Os is within the range of concentrations observed in the basalts with the lowest MgO

442 analysed in this study (5-44 ppt for MgO 5.1-8.7 wt.%), some of the latter presenting  
443 phenocryst assemblages with up to 70% plagioclase and less than 20% olivine (e.g.  
444 STV324; Heath et al. (1998)).

445 All data could be modeled using the same starting (LAG-4) and assimilant  
446 composition (Table 3) and with  $F > 0.8$ . In  $^{87}\text{Sr}/^{86}\text{Sr}$  vs.  $^{187}\text{Os}/^{188}\text{Os}$  space, the lavas fall  
447 on two trends produced by different rates of assimilation and small variations in  $D_{\text{Sr}}$  ( $r =$   
448  $0.56$  vs.  $0.70$ ;  $D_{\text{Sr}} = 1.4$ - $1.8$ ). On trace element ratio vs. isotope diagrams (Fig.6b, c), the  
449 effect of variations in the fractionating assemblage during assimilation on different  
450 islands (= variation in  $D$ ) is reflected by small displacement of the samples on these  
451 trends compared to isotope-isotope space (Fig. 6a). The north-south difference observed  
452 in  $\text{La}/\text{Sm}$  vs.  $^{187}\text{Os}/^{188}\text{Os}$  can be easily produced by increasing  $D_{\text{La}/\text{Sm}}$ . We suggest that  
453 such north-south variations in  $D_{\text{La}/\text{Sm}}$  could be related to the depth at which AFC occurs.  
454 In this case, the assemblage fractionated during assimilation in the north of the arc  
455 depleted La less than the assemblage fractionated in the south for a constant  $D_{\text{Sm}}$ . For  
456 example, it would be the case if, during assimilation, the fractionated assemblage is  
457 dominated by olivine ( $D_{\text{La}/\text{Sm}} \sim 1$ ) in the south of the arc and by clinopyroxene ( $D_{\text{La}/\text{Sm}} < 1$ )  
458 in the north of the arc. Such variations in the fractionating assemblage composition would  
459 have negligible effect on the isotopic composition of the lavas, consistent with the single  
460 trend observed in Sr vs Os isotopes from north to south.

#### 461 **4.4 Implications**

##### 462 *4.4.1 The Lesser Antilles*

463           Although assimilation of sediment (high  $\delta^{18}\text{O}$ ,  $^{87}\text{Sr}/^{86}\text{Sr}$ ,  $^{208-207-206}\text{Pb}/^{204}\text{Pb}$  and low  
464  $^{176}\text{Hf}/^{177}\text{Hf}$  and  $^{143}\text{Nd}/^{144}\text{Nd}$  ratios) had been shown to modify some lava compositions in  
465 the central-southern part of the arc (Thirlwall and Graham, 1984; Davidson, 1987;  
466 Davidson and Harmon, 1989; Smith et al., 1996; Thirlwall et al., 1996; Van Soest et al.,  
467 2002; Bezard et al., 2014), assimilation of another component in the deep crust of the  
468 Lesser Antilles arc (Fig. 7) was not anticipated and differences between the Grenada  
469 picrite compositions and the rest of the arc lavas have traditionally been attributed to  
470 differences in source composition. This work suggests that the Grenada picrites might  
471 provide the only close estimates of the source composition in terms of  $^{87}\text{Sr}/^{86}\text{Sr}$ ,  
472  $^{187}\text{Os}/^{188}\text{Os}$ , Sr and REE. Thus, the use of such proxies in less primitive lavas to constrain  
473 the relative contributions of fluids versus sediment in the arc source may need  
474 reappraisal. All the arc data seem to back-project toward a primitive magma with the  
475 Grenada picrite composition (Fig. 4) although small variations in the source from north to  
476 south can't be precluded. The investigation of such variations is, however, hampered by  
477 the absence of very mafic lavas, such as those found in St Vincent and Grenada, in the  
478 northern arc. Since the Grenada picrite is the only silica undersaturated lavas, this  
479 suggests that primitive magma along the arc in general could be of a similar alkaline  
480 nature before AFC, as suggested by Macdonald et al. (2000). The absence of cumulate  
481 assimilation by Grenada picrites could be either due to a lack of significant amount of  
482 cumulate at the base of the arc crust, or to the presence of crustal structures allowing the  
483 magma to reach the surface with minimal stalling at the base of the crust. The latter  
484 hypothesis could be supported by the presence of a transform fault in Grenada, which has  
485 been suggested to control the emplacement of the most recent products (Arculus, 1976).

486 4.4.2 *Other arcs*

487 The correlation between Os (or 1/Os) and  $^{187}\text{Os}/^{188}\text{Os}$  observed in the Lesser  
488 Antilles arc is not unique and has been noted in most continental and oceanic arc lavas  
489 (Fig. 8a; Alves et al., 1999; 2002; Borg et al., 2000; Chesley et al. 2002; Woodland et al.,  
490 2002; Woodhead et al., 2004; Turner et al., 2009; Righter et al., 2012). However, clear  
491 correlations between Os isotopes and both Os concentrations and indices of  
492 differentiation (MgO, SiO<sub>2</sub>) have only been noted in continental arcs (Lassiter and Luhr,  
493 2001; Chesley et al., 2002). The absence of clear MgO-SiO<sub>2</sub> correlations with  $^{187}\text{Os}/^{188}\text{Os}$   
494 in oceanic arc lavas (Fig. 8b) led previous studies to suggest source control of the inverse  
495 correlation between Os concentration and  $^{187}\text{Os}/^{188}\text{Os}$  (Alves et al., 1999). Our Lesser  
496 Antilles study suggests that the correlations between  $^{187}\text{Os}/^{188}\text{Os}$  and Os content and the  
497 “radiogenic  $^{187}\text{Os}/^{188}\text{Os}$  ratios observed in oceanic arcs could reflect crustal assimilation  
498 and that slab-derived Os may not be transferred into the magma source regions, as  
499 proposed by Righter et al. (2012). It also suggests, based on the radiogenic  $^{187}\text{Os}/^{188}\text{Os}$   
500 ratio in the St Vincent high-MgO lavas (MgO = 12.6 wt. %), that the process can affect  
501 very primitive magmas. Although the conditions of assimilation may be different in every  
502 arc, early assimilation during differentiation could explain the radiogenic  $^{187}\text{Os}/^{188}\text{Os}$   
503 observed in early crystallizing phases such as Cr-spinel in Bonin Islands tholeiites  
504 (Suzuki et al, 2011).

505 Unlike the correlation between Os isotopes and Os concentrations, the covariation  
506 of Os isotopes with lithophile isotope or trace element ratios observed in the Lesser  
507 Antilles (e.g. Sr isotopes, Sr/Th and La/Sm) is not ubiquitous in other arcs (e.g. Fig. 8c,  
508 d), with only the Cascades lavas showing similarly clear correlations between  $^{187}\text{Os}/^{188}\text{Os}$



509 and  $^{87}\text{Sr}/^{86}\text{Sr}$  ratios and Sr concentrations (Borg et al., 2000; Fig. 8c, d). This lack of  
510 obvious co-variation could be explained by more limited compositional differences  
511 between the primary magma and the assimilant which would rend the impact of  
512 assimilation harder to observe. Indeed, in the Lesser Antilles, the  $^{87}\text{Sr}/^{86}\text{Sr}$ , Sr/Th and  
513 La/Sm ratios of the primitive magmas differs significantly from those of the assimilant,  
514 which results in obvious mixing lines. However, the  $^{87}\text{Sr}/^{86}\text{Sr}$ , Sr/Th and La/Sm ratios of  
515 primitive magmas are likely to vary with the composition of the subducted sediment and  
516 as demonstrated in Fig. 8c and 8d, the very ‘continental’ isotopic and trace element  
517 signature of the Lesser Antilles primitive magma is not commonly observed in other  
518 oceanic arcs, the latter presenting composition closer to MORB (e.g. picrites from the  
519 Vanuatu or Salomon islands have  $^{87}\text{Sr}/^{86}\text{Sr} \sim 0.703\text{-}0.7045$  contrasting with the  $^{87}\text{Sr}/^{86}\text{Sr}$   
520 of  $\sim 0.7051$  of the most primitive picrite in Grenada; Peate et al., 1997; Schuth et al.,  
521 2004). Therefore, assimilation of a recent FAB like cumulate by primitive magmas would  
522 be much harder to detect in most oceanic arcs than in the Lesser Antilles. In addition, the  
523 rocks assimilated in other arcs might have lower Sr concentrations, rending the impact of  
524 the process on Sr/Th and  $^{87}\text{Sr}/^{86}\text{Sr}$  hard to fingerprint. Alternatively, along-arc primitive  
525 magma compositional variations may exist, interfering with the variations produced by  
526 assimilation.

## 527 **5. CONCLUSIONS**

528 Our observations suggest that no significant slab derived Os is present in the  
529 primitive magmas of the Lesser Antilles arc. We interpret the increase in Os isotopic  
530 ratios observed in the lavas as caused by crustal assimilation in the deep crust of the arc.  
531 The assimilant would be similar all along the arc and display lower  $^{87}\text{Sr}/^{86}\text{Sr}$  (MORB-

532 like), La/Sm and higher  $^{187}\text{Os}/^{188}\text{Os}$ , Sr and Sr/Th than the primitive magma. We suggest  
533 that it could be a plagioclase-rich cumulate present at the base of the arc. Such cumulate  
534 could have been produced during the early-arc stage, prior to significant amount of  
535 fluids/sediments fluxing in the mantle.

#### 536 **ACKNOWLEDGEMENTS**

537 Financial support was provided to Rachel Bezar by Durham and Macquarie  
538 University cotutelle studentship (No. 2012060). We thank Peter Wieland for his help  
539 during the analytical work and we thank Matthijs C. van Soest for providing some of the  
540 samples.

#### 541 **REFERENCES**

- 542 Alves, S., Schiano, P. and Allegre, C.J. (1999) Rhenium-osmium isotopic investigation of  
543 Java subduction zone lavas. *Earth Planet. Sci. Lett.* **168**, 65-77.
- 544 Alves, S., Schiano, P., Capmas, F. and Allegre, C.J. (2002) Osmium isotope binary  
545 mixing arrays in arc volcanism. *Earth Planet. Sci. Lett.* **198**, 355-369.
- 546 Arculus, R. (1976) Geology and geochemistry of the alkali basalt-andesite association of  
547 Grenada. Lesser Antilles island arc. *Geol. Soc. Am. Bull.* **87**, 612-624.
- 548 Bezar, R., Davidson, J.P., Turner, S., Macpherson, C.G., Lindsay, J.M. and Boyce, A.J.,  
549 (2014) Assimilation of sediment embedded in oceanic arc crust: myth or reality? *Earth*  
550 *Planet. Sci. Lett.* **395**, 51-60.
- 551 Baker, P.E. (1984) Geochemical evolution of St Kitts and Montserrat, Lesser Antilles. *J.*  
552 *Geol. Soc. Lond.* **141**, 401-411.

553 Borg, L.E., Brandon, A.D., Clyne, M.A. and Walker, R.J. (2000) Re-Os isotopic  
554 systematics of primitive lavas from the Lassen region of the Cascade Arc, California.  
555 *Earth Planet. Sci. Lett.* **177**, 301-317.

556 Boynton, C.H., Westbrook, G.K., Bott, M.H.O. and Long, R.E., 1979. A seismic  
557 refraction investigation of crustal structure beneath the Lesser Antilles island arc.  
558 *Geophys. J. R. Astron. Soc.* **58**, 371-393.

559 Brandon, A.D. and Draper, D.S. (1996) Constraints on the origin of the oxidation state of  
560 the mantle overlying subduction zones: an example from Simcoe, Washington, USA.  
561 *Geochim. Cosmochim. Acta* **60**, 1739-1749.

562 Brandon, A.D., Creaser, R.A., Shirey, S.B. and Carlson, R.W. (1996) Os recycling in  
563 subduction zones. *Science* **272**, 861-864.

564 Brounce, M.N., Kelley, K. and Cottrell, E. (2013) Temporal evolution of  $fO_2$  in the  
565 Mariana mantle wedge. *American Geophysical Union abstract*.

566 Carpentier, M., Chauvel, C. and Mattielli, N. (2008) Pb-Nd isotopic constraints on  
567 sedimentary input into the Lesser Antilles arc system. *Earth Planet. Sci. Lett.* **272**, 199-  
568 211.

569 Chesley, J., Ruiz, J., Richter, K., Ferrari, L. and Gomez-Tuena, A. (2002) Source  
570 contamination versus assimilation: an example from the Trans-Mexican Volcanic Arc.  
571 *Earth Planet. Sci. Lett.* **195**, 211-221.

572 Cohen, A.S. and Waters, F.G. (1996) Separation of osmium from geological materials by  
573 solvent extraction for analysis by thermal ionisation mass spectrometry. *Anal. Chim. Acta*  
574 **332**, 269-275.

575 Creaser, R.A., Papanastassiou, D.A. and Wasserburg, G.J. (1991) Negative thermal ion  
576 mass spectrometry of osmium, rhenium and iridium. *Geochim. Cosmochim. Acta* **55**, 397-  
577 401.

578 Davidson, J.P. (1984) Petrogenesis of Lesser Antilles island arc magmas: Isotopic and  
579 geochemical constraints. *PhD thesis, Uni. Leeds*, 308 pp.

580 Davidson, J.P. (1986) Isotopic and trace element constraints on the petrogenesis of  
581 subduction-related lavas from Martinique, Lesser Antilles. *J Geophys. Res.* **91**, 5943-  
582 5962.

583 DePaolo, D.J. (1981) Trace element and isotopic effects of combined wall rock  
584 assimilation and fractional crystallization. *Earth Planet. Sci. Lett.* **53**, 189-202.

585 Dufrane, S.A., Turner, S., Dosseto, A. and Van Soest, M. (2009) Reappraisal of fluid and  
586 sediment contributions to Lesser Antilles magmas. *Chem. Geol.* **265**, 272-278.

587 Germa, A., Quidelleur, X., Labanieh, S., Chauvel, C. and Lahitte, P. (2011) The Volcanic  
588 evolution of Martinique Island: Insights from K-Ar dating into the Lesser Antilles arc  
589 migration since the Oligocene. *J. volcano. Geoth. Res.* **208**, 122-135.

590 Hart, S.R. and Davis, K.E. (1978). Nickel partitioning between olivine and silicate melt.  
591 *Earth and Planet. Sci.* **40**, 203-209.

592 Hayes, D.E., et al. (1972) Initial Reports of the Deep Sea Drilling Project 14. U.S.  
593 Government Printing Office, Washington.

594 Heath, E., Macdonald, R., Belkin, H., Hawkesworth, C. and Sigurdsson, H. (1998)  
595 Magmagenesis at Soufriere Volcano, St Vincent, Lesser Antilles Arc. *J. Petrology* **39**,  
596 1721-1764.

597 Kendall, B., Creaser, R.A. and Selby, D. (2009)  $^{187}\text{Re}$ - $^{187}\text{Os}$  geochronology of  
598 Precambrian organic-rich sedimentary rocks. *Geol. Soc. London Spec. Pub.* **326**, 85-107.

599 Le Guen de Kerneizon, M., Carron, J.P., Bellon, H. and Maury, R.C. (1981). Enclaves  
600 metamorphiques et plutoniques, provenant du substratum des Petites Antilles, dans les  
601 formations volcaniques de l'île de Sainte Lucie. *CR Acad. Sci. Paris* **292**, 899-902.

602 Macdonald, R., Hawkesworth, C.J. and Heath, E. (2000) The Lesser Antilles volcanic  
603 chain: a study in arc magmatism. *Earth Sci. Rev.* **49**, 1-76.

604 McInnes, B.I.A., McBride, J.S., Evans, N.J., Lambert, D.D. and Andrew, A.S. (1999)  
605 Osmium Isotope Constraints on Ore Metal Recycling in Subduction zones. *Science* **286**,  
606 512.

607 Nowell, G.M., Luguet, A., Pearson, D.G. and Horstwood, M.S.A. (2008). Precise and  
608 accurate  $^{186}\text{Os}/^{188}\text{Os}$  and  $^{187}\text{Os}/^{188}\text{Os}$  measurements by multi-collector plasma ionisation  
609 mass spectrometry (MC-ICP-MC) part I: Solution analyses. *Chem. Geol.* **248**, 363-393.

610 Parkinson, J.J., Hawkesworth, C.J. and Cohen, A.S. (1998) Ancient mantle in a modern  
611 arc: osmium isotopes in Izu-Bonin-Mariana forearc peridotites. *Science* **281**, 2011-2013.

612 Peate, D.W., Pearce, J.A., Hawkesworth, C.J., Colley, H., Edwards, C.M.H. and Hirose,  
613 K. (1997) Geochemical variations in Vanuatu Arc lavas: the role of the subducted  
614 material and a variable mantle wedge composition. *J. petrol.* **38**, 1331-1358.

615 Penniston-Dorland, S.C., Walker, R.J., Pitcher, L., Sorensen, S.S. (2012) Mantle-crust  
616 interactions in a paleosubduction zone: Evidence from a highly siderophile element  
617 systematics of eclogite and related rocks. *Earth Planet. Sci. Lett.* **319-320**, 295-306.

618 Penniston-Dorland, S.C., Gorman, J.K., Bebout, G.E., Piccoli, P.M. and Walker, R.J.  
619 (2014) Reaction rind formation in the Catalina Schist: Deciphering a history of  
620 mechanical mixing and metasomatic alteration. *Chem. Geol.* **384**, 47-61.

621 Peucker-Ehrenbrink, B. and Ravizza, G. (2000) The marine osmium isotope record.  
622 *Terra Nova* **12**, 205-219.

623 Reagan, M.K., Ishizuka, O., Stern, R.J., Kelley, K.A., Ohara, Y. et al. (2010) Fore-arc  
624 basalts and subduction initiation in the Izu-Bonin-Mariana system. *Geochem. Geophys.*  
625 *Geosyst.* **Q03X12**, doi: 10.1029/2009GC002871.

626 Righter, K., Chesley and J.T. and Ruiz, J. (2002) Genesis of primitive, arc type basalt:  
627 Constraints from Re, Os, and Cl on the depth of melting and role of fluids. *Geology* **30**,  
628 619-622.

629 Rudnick, R. and Walker, R.J. (2009) Interpreting ages from Re-Os isotopes in peridotites.  
630 *Lithos* **102S**, 1083-1095.

631 Saal, A.E., Rudnick, R.L., Ravizza, G.E. and Hart, S.R. (1998) Re-Os isotope evidence  
632 for the composition, formation and age of the lower continental crust. *Lett. Nature* **393**,  
633 58-61.

634 Salters, V.J.M. and Stracke, A. (2004) Composition of the depleted mantle. *Geochem.*  
635 *Geophys. Geosyst* **Q05B07**, doi: 10.1029/2003GC000597.

636 Schuth, S., Rohrbach, A., Munker, C., Ballaus, C., Garbe-Schonberg, D. and Qopoto, C.  
637 (2004) Geochemical constraints on the petrogenesis of arc picrites and basalts, New  
638 Georgia Group, Solomon Islands. *Contrib. Mineral. Petrol.* **148**, 288-304.

639 Selby, D. and Creaser, R.A. (2003) Re-Os geochronology of organic-rich sediments: an  
640 evaluation of organic matter analysis methods. *Chem. Geol.* **200**, 225-240.

641 Sun, S.S. and McDonough, W.F. (1989) Chemical and isotopic systematics of oceanic  
642 basalts: implications for mantle composition and processes. *Geol. Soc. Lond.* **42**, 313-  
643 345.

644 Suzuki, K., Senda, R. and Shimizu, K. (2011) Osmium behaviour in a subduction system  
645 elucidated from chromian spinel in Bonin Island beach sands. *Geology* **39**, 999-1002.

646 Senda, R., Tanaka, T. and Suzuki, K. (2007) Os, Nd and Sr isotopic and chemical  
647 compositions of ultramafic xenoliths from Kurose, SW Japan: Implications for  
648 contribution of slab-derived material to wedge mantle. *Lithos* **95**, 229-242. Turner, S.,  
649 Handler, M., Bindeman, I. and Suzuki, K. (2009) New insights into the origin of O-Hf-Os  
650 isotope signatures in arc lavas from Tonga-Kermadec. *Chem. Geol.* **266**, 187-193.

651 Thirlwall, M.F., Graham, A.M., Arculus, R.J., Harmon, R.S. and Macpherson, C.G.  
652 (1996) Resolution of the effects of crustal assimilation, sediment subduction and fluid  
653 transport in island arc magmas: Pb-Sr-Nd-O isotope geochemistry of Grenada, Lesser  
654 Antilles. *Geochim. Cosmochim. Acta* **60**, 4785-4810.

655 Turgeon, S. and Creaser, R.A. (2008) Cretaceous oceanic anoxic event 2 triggered by a  
656 massive magmatic episode. *Nature* **454**, 323-326.

657 Van Soest, M. C. (2000) Sediment Subduction and Crustal contamination in the Lesser  
658 Antilles Island Arc. PhD thesis Uni. Vrije, 287 pp.

659 Volkening, J., Walczyk, T. and Heumann, K.G. (1991) Osmium isotope ratio  
660 determinations by negative thermal ionization mass spectrometry. *Int. J. Mass Spec. Ion*  
661 *Process.* **105**, 147-159.

662 Widom, E., Kepezhinskas, P. and Defant, M. (2003) The nature of metasomatism in the  
663 sub-arc mantle wedge: evidence from Re-Os isotopes in Kamchatka peridotite xenoliths.  
664 *Chem. Geol.* **196**, 283-306.

665 Woodhead, J. and Brauns, M. (2004) Current limitations to the understanding of Re-Os  
666 behaviour in subduction systems, with an exemple from New Britain. *Earth Planet. Sci.*  
667 *Lett.* **221**, 309-323.

668 Woodland, S.J., Pearson, D.G. and Thirlwall, M.F. (2002) A Platinum Group Element  
669 and Re-Os Isotope Investigation of Siderophile Element Recycling in Subduction Zones:  
670 Comparison of Grenada, Lesser Antilles Arc, and the Izu-Bonin Arc. *J. Petrol.* **43**, 171-  
671 198.



672 Xiong, Y. and Wood, S.A. (1999) Experimental determination of the solubility of ReOs  
673 and the dominant oxidation state of rhenium in hydrothermal systems. *Chem. Geol.* **158**,  
674 245-256.

675 Xiong, Y. and Wood, S.A. (2000) Experimental quantification of hydrothermal solubility  
676 of platinum group elements with special reference to porphyry copper environments.  
677 *Mineral. Petrol.* **68**, 1-28.

678 **Figure captions:**

679 Fig. 1: Map of the Lesser Antilles arc with the location of selected lava samples (in  
680 black). One sample from each island (except St. Vincent, n=2) was analysed. See Table 1  
681 for sample identification. The latitude of DSDP sites 543/543A and 144 are also  
682 indicated.

683 Fig. 2:  $^{87}\text{Sr}/^{86}\text{Sr}$  vs. (a)  $^{143}\text{Nd}/^{144}\text{Nd}$ , (b) MgO (wt. %), (c) La/Sm and (d) Sr/Th of the  
684 lavas selected. Data presented in Table 2.

685 Fig. 3: Os (ppb) vs.  $^{187}\text{Os}/^{188}\text{Os}$  of the arc lavas and the subducting slab. DMM =  
686 Depleted MORB mantle from Rudnick and Walker (2009). Note logarithmic scales. Data  
687 presented in Table 1.

688 Fig. 4: Lavas Os (ppb) and MgO (wt. %) against  $^{187}\text{Os}/^{188}\text{Os}$ . Same legend as in figure 3.  
689 The same negative correlation is also observed between  $^{187}\text{Os}/^{188}\text{Os}$  and Mg#. Woodland  
690 et al. (2002) data on different Grenada lavas are shown for comparison. Arrows shows  
691 potential differentiation trends for the northern and southern islands, starting with the  
692 most primitive lava of the arc.

693 Fig. 5: (a)  $^{87}\text{Sr}/^{86}\text{Sr}$ , (b) La/Sm and (c) Sr/Th vs  $^{187}\text{Os}/^{188}\text{Os}$  composition of the lavas.  
694 Subducting slab composition are also indicated. Data for arc lavas and sediment and  
695 altered basalt from the slab are presented in Tables 1 and 3. DMM = depleted mantle  
696 from Rudnick and Walker (2009) for Os isotopes and Salters and Stracke (2004) for Sr.  
697 isotopes; Lower continental crust composition is from Saal et al. (1999), N-MORB trace  
698 element composition is from Sun and McDonough (1989). Arrows highlight the negative  
699 trends drawn by the data.

700 Fig. 6: Assimilation during Fractional Crystallization (AFC) models of (a,b)  $^{87}\text{Sr}/^{86}\text{Sr}$ ,  
701 (a,c)  $^{187}\text{Os}/^{188}\text{Os}$ , (b) Sr/Th and (c) La/Sm ratios of the Lesser Antilles primitive lavas  
702 using DePaolo (1981) equation. Parameters for Models 1 and 2 are shown in Table 3.  
703 Dots represent the fraction of melt remaining (F). In (b) and (c), samples with  
704 compositions displaced from their position on the trends defined in the isotope-isotope  
705 space (a) (likely due to the impact of mineral fractionation) are circled. The arrows show  
706 the inferred compositions before displacements.

707 Fig. 7: Schematic model for the Lesser Antilles plumbing system to explain the main  
708 factors influencing the compositional variations of the arc lavas. The figure illustrates  
709 both the locus (cartoon) and the impact (diagrams) of cumulate assimilation on the lava's  
710  $^{187}\text{Os}/^{188}\text{Os}$ ,  $^{87}\text{Sr}/^{86}\text{Sr}$ , La/Sm and  $\delta^{18}\text{O}$  compositions (evolution of Sr/Th ratio is not  
711 shown). The impact of subsequent assimilation of sediment (Bezard et al., 2014), which  
712 is not discussed in this contribution, is also shown for a full illustration of the arc  
713 processes. The arc primary magmas would come from a source strongly influence by the  
714 subducted sediment. Grenada picrite (A) would have avoided any storage in the arc crust  
715 and retained the primitive magma composition. All the less primitive lavas (B) would

716 have spent variable amounts of time in contact with a plagioclase-rich cumulate in the  
717 lower parts of the crust. The resulting magmas would have either ascended directly to the  
718 surface (B) or assimilated some sediment during the ascent (C). M = mantle composition.

719 Fig. 8: Comparison of the Lesser Antilles arc lava compositions with those of other arcs  
720 (continental and oceanic). The negative correlation observed between Os isotopes and Os  
721 concentrations is ubiquitous in arcs (a). On the other hand, negative correlations between  
722 Os isotopes and MgO (b) or Sr isotopes (c) as well as a positive correlation between  
723 Sr/Th and Os isotopes (d) are not observed in every arcs. Lava compositions are from  
724 Borg et al., (2000) for the Cascades, Chesley et al. (2002) for the Trans-Mexican arc,  
725 Turner et al. (2009) for the Tonga-Kermadec, Alves et al. (1999) for Java, Woodhead and  
726 Brauns (2004) for New Britain and Woodland et al. (2002) for the additional Lesser  
727 Antilles arc data.

728

Fig. 1

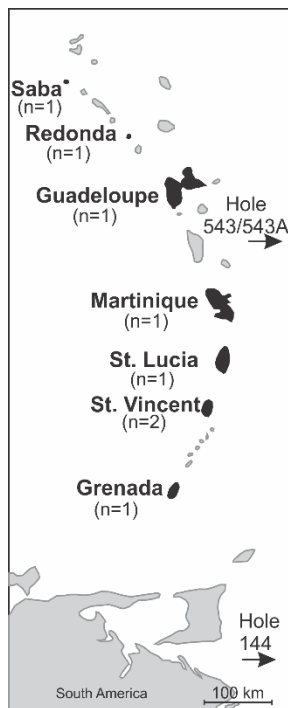


Fig. 2

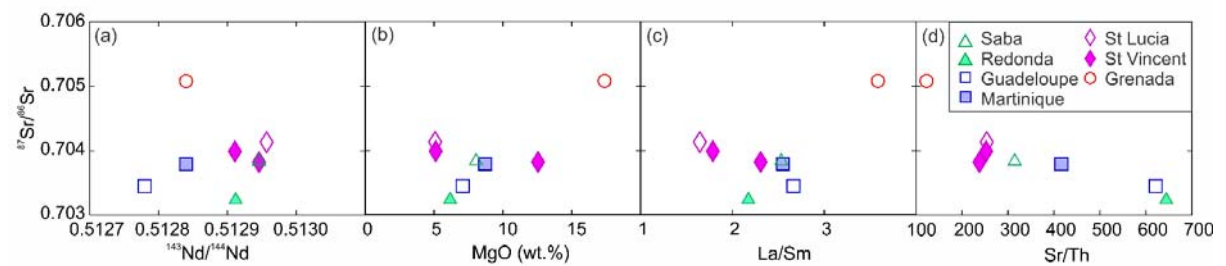


Fig. 3

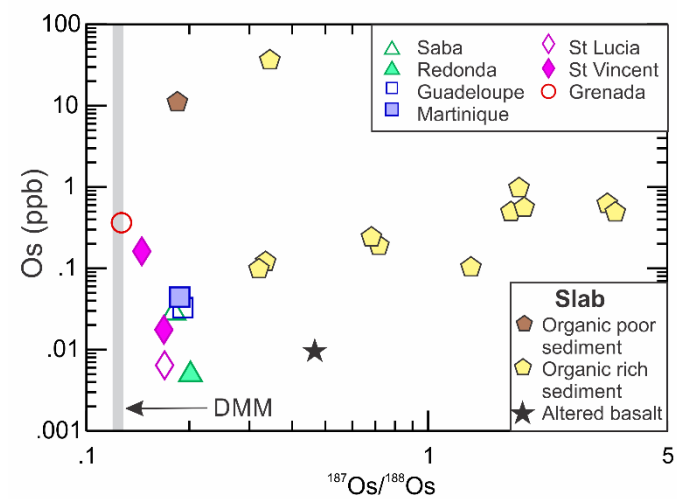


Fig. 4

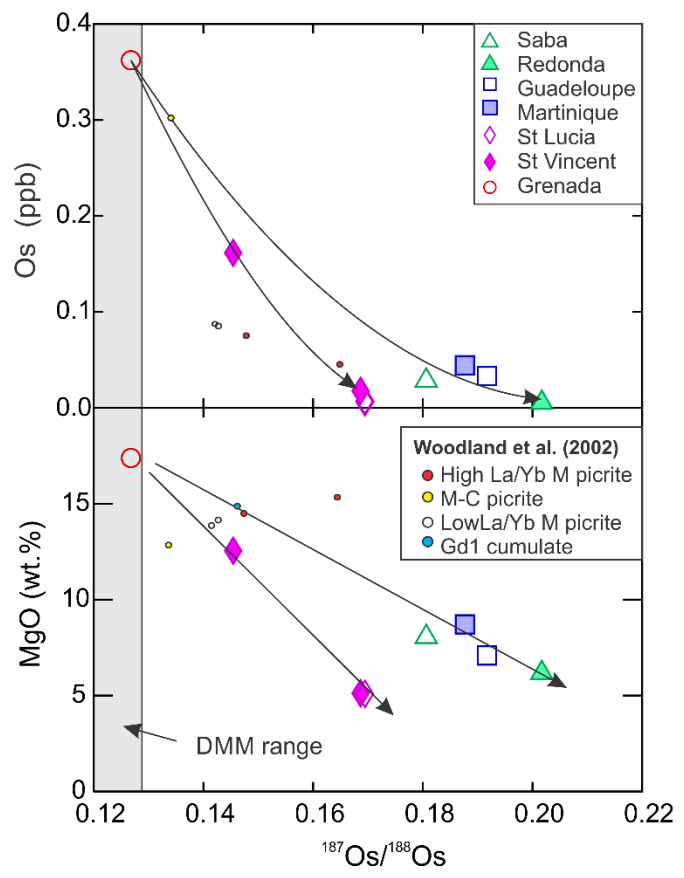


Fig. 5

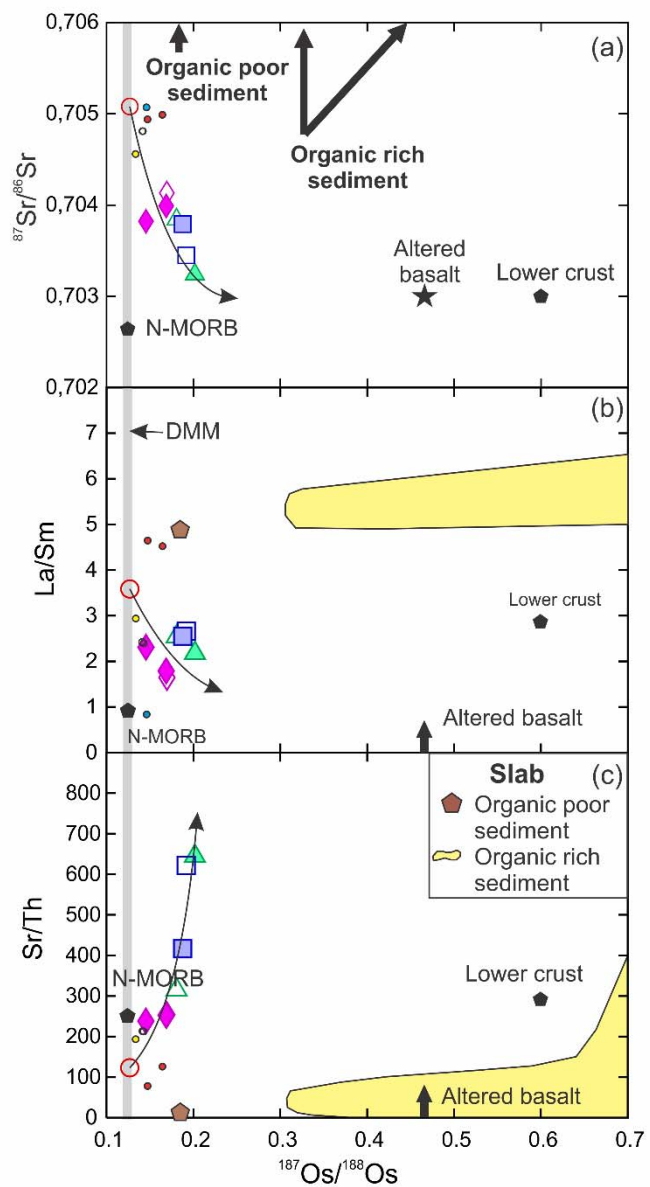


Fig. 6

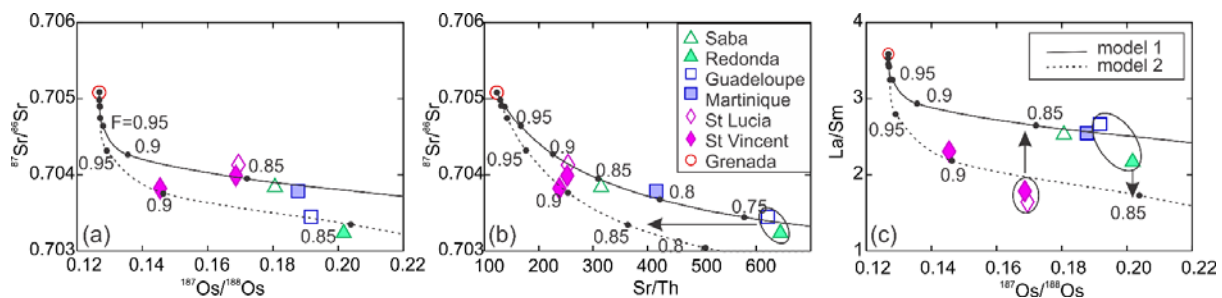


Fig. 7

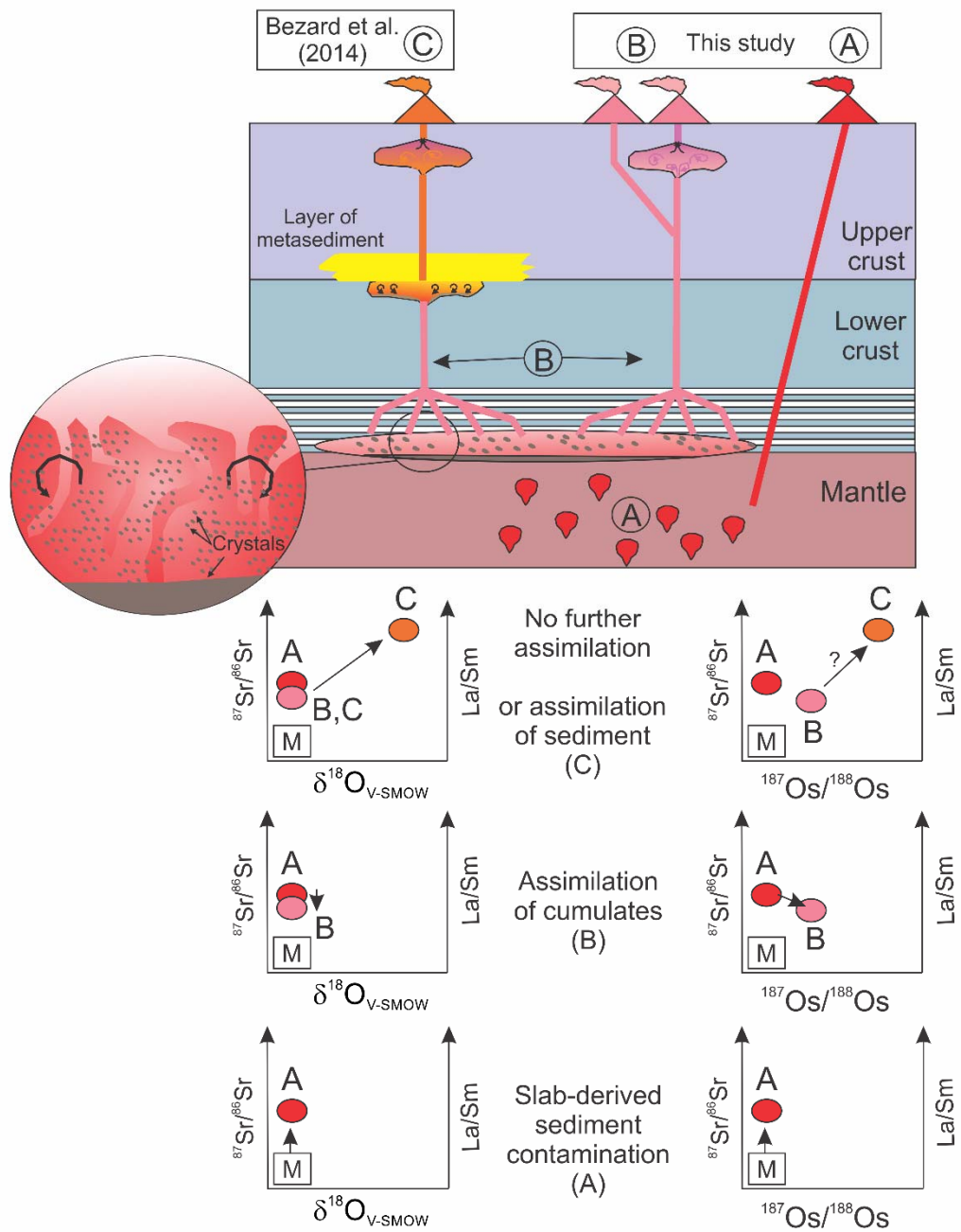
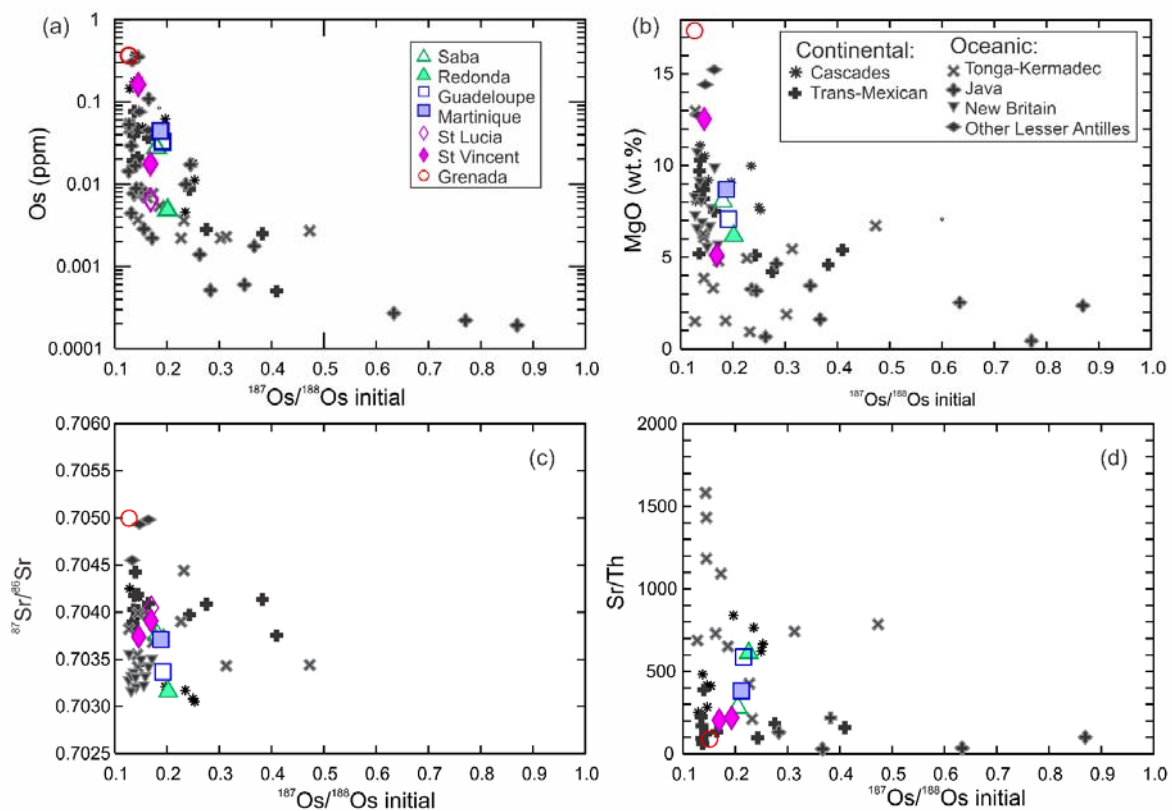


Fig. 8





**Table 1: Os data for the arc lavas and altered basalt and sediments from the subducting slab.**

	Subbottom depth (m)	Lithology Unit #	Os (ppb)	±	<sup>187</sup> Os/ <sup>188</sup> Os	±	<sup>187</sup> Re/ <sup>188</sup> Os	±	Re (ppb)	±	Age (ka) <sup>d</sup>	<sup>187</sup> Os/ <sup>188</sup> Os initial
<b>Lavas (from N to S):</b>												
Saba-LAS1 <sup>a</sup>	–	–	0.0281	0.0001	0.181	0.001	–	–	–	–	<10	–
Redonda-R8204 <sup>a</sup>	–	–	0.0049	0.0001	0.202	0.002	–	–	–	–	1000	–
Guadeloupe-GUAD510 <sup>a</sup>	–	–	0.0328	0.0004	0.192	0.001	–	–	–	–	500	–
Martinique-M8328 <sup>a</sup>	–	–	0.0441	0.0002	0.188	0.001	–	–	–	–	<1000	–
St Lucia-SL8344 <sup>a</sup>	–	–	0.0064	0.0001	0.170	0.005	–	–	–	–	11400	–
St Vincent-STV301 <sup>a</sup>	–	–	0.161	0.001	0.1451	0.0007	–	–	–	–	180	–
St Vincent-STV324 <sup>a</sup>	–	–	0.0175	0.0001	0.169	0.002	–	–	–	–	<3.6	–
Grenada-LAG4 <sup>a</sup>	–	–	0.362	0.001	0.1268	0.0004	–	–	–	–	<10	–
Altered basalt 543 16 5 20-24 <sup>a</sup>	–	–	0.0096	0.0002	0.466	0.003	–	–	–	–	–	–
<b>Sediments (increasing depth):</b>												
<b>Site DSDP 543</b>												
78A-543-17-3-120-124 <sup>b</sup>	166	3	11.2	0.4	0.185	0.007	–	–	–	–	16000	–
<b>Site DSDP 144/144A</b>												
14-144A-5-1 interval 123-124 <sup>c</sup>	181	3	0.1009	0.0008	1.33	0.02	389	5	7.03	0.03	85000	0.78
14-144A-6-1 interval 70-110 <sup>c</sup>	189	3	0.941	0.003	1.844	0.005	721	3	115.0	0.4	89000	0.77
14-144Z-4-2 interval 60-64 <sup>c</sup>	215	3	0.478	0.003	3.52	0.02	1494	8	102.8	0.3	93000	1.21
14-144Z-4-2 interval 143-146 <sup>c</sup>	216	3	0.602	0.003	3.34	0.01	1425	6	125.4	0.4	93000	1.13
14-144Z-4-3 interval 31-33 <sup>c</sup>	216	3	0.534	0.002	1.913	0.006	755	3	67.8	0.2	93000	0.74
14-144Z-4-3 interval 100-103 <sup>c</sup>	217	3	0.484	0.002	1.746	0.007	580	3	48.1	0.2	93000	0.85
14-144Z-5-1 interval 5-6 <sup>c</sup>	264	4	0.231	0.001	0.682	0.008	178	2	7.93	0.03	98000	0.39
14-144Z-5-1 interval 143-143 <sup>c</sup>	265	4	0.186	0.002	0.72	0.02	164	3	5.89	0.02	98000	0.45
14-144Z-7-1 interval 136-137 <sup>c</sup>	299	5	0.116	0.001	0.34	0.01	32.3	0.7	0.757	0.007	106000	0.28
14-144Z-7-1 interval 123-124 <sup>c</sup>	299	5	34.5	0.3	0.34	0.01	122	3	847	3	106000	0.13
14-144Z-8-3 interval 136-137 <sup>c</sup>	328	5	0.0934	0.0005	0.321	0.005	16.7	0.7	0.32	0.01	113000	0.29

<sup>a</sup> Os, <sup>187</sup>Os/<sup>188</sup>Os analysed at Macquarie University.

<sup>b</sup> Organic poor sediment: Os, <sup>187</sup>Os/<sup>188</sup>Os analysed at Macquarie University.

<sup>c</sup> Organic rich sediment: Os, <sup>187</sup>Os/<sup>188</sup>Os, Re analysed at Durham University

<sup>d</sup> Ages of Lava flows were taken from the following sources: Saba (Dufrane et al. 2009); Redonda (Baker, 1984); Guadeloupe (Dufrane et al., 2009); Martinique, Carbet Complex (Germa et al. (2011); St Lucia, Anse Galet (Le Guen de Kerneizon et al. (1983); St Vincent (Heath et al. (1998); Grenada (Dufrane, 2009). Ages indicated for the sediments, also used to calculate the initial <sup>187</sup>Os/<sup>188</sup>Os ratios, correspond to that of the samples analysed by Carpentier et al. (2008; 2009) named in Table 2.

Note: Uncertainties are given as 2 sigma. For the latter the uncertainty includes the 2SE uncertainty for mass spectrometer analysis plus uncertainties for Os blank abundance and isotopic composition. The external reproducibility for <sup>187</sup>Os/<sup>188</sup>Os and Os in lavas and organic-poor sediment, based on replicate analyses of WPR-1, is 1% and 4%, respectively. The external reproducibility for <sup>187</sup>Os/<sup>188</sup>Os, <sup>187</sup>Re/<sup>188</sup>Os, Os and Re in organic rich sediments, based on replicate analyses of SDO-1, is 7%, 7%, 16% and 15% respectively (see section 2.2).

**Table 2: Lithophile major and trace element concentrations and isotopes of the arc lavas and altered basalt and sediments from the subducting slab analysed.**

	Sample used for sediment lithophile element compositions (Carpentier et al., 2008;2009)	Subbotom Depth	MgO (wt. %)	Mg#	Sr (ppm)	La (ppm)	Sm (ppm)	Th (ppm)	<sup>87</sup> Sr/ <sup>86</sup> Sr	<sup>143</sup> Nd/ <sup>144</sup> Nd	
<b><u>Lavas (from N to S):</u></b>											
	Saba-LAS1 <sup>a</sup>	–	8.05	0.82	321	5.8	2.29	1.02	0.70384	0.51295	
	Redonda-R8204 <sup>a</sup>	–	6.17	0.74	493	4	1.84	0.77	0.70324	0.51291	
	Guadeloupe-GUAD510 <sup>a</sup>	–	7.08	0.76	261	3.7	1.4	0.42	0.70345	0.51278	
	Martinique-M8328 <sup>a</sup>	–	8.71	0.83	358	5.2	2.04	0.86	0.70379	0.51284	
	St Lucia-SL8344 <sup>a</sup>	–	5.08	0.69	177	3.3	2.03	0.70	0.70413	0.51296	
	St Vincent-STV301 <sup>a</sup>	–	12.55	0.86	202	5.7	2.47	0.85	0.70382	0.51295	
	St Vincent-STV324 <sup>a</sup>	–	5.12	0.74	236	4.9	2.72	0.94	0.70399	0.51291	
	Grenada-LAG4 <sup>a</sup>	–	17.38	0.89	296	9.3	2.6	2.41	0.70508	0.51284	
	Altered basalt 543 16 5 20-24 <sup>a</sup>	–	–	–	–	–	3.36	–	0.70304	0.51312	
<b><u>Sediment (increasing depth):</u></b>											
<b>Site DSDP 543:</b>											
	78A-543-17-3-120-124 <sup>b</sup>	543 18 4W 15-17	174	2.91	–	83	23.5	4.83	8.69	0.714076	0.51207
<b>Site DSDP 144/144A:</b>											
	14-144A-5-1 interval 123-124 <sup>b</sup>	144A 5 1W 119-124	181	0.78	–	750	10.4	1.46	2.31	0.707871	0.51184
	14-144A-6-1 interval 70-110 <sup>b</sup>	144A 6 1W 90-93	190	0.77	–	681	11.5	1.56	2.16	0.707884	0.51183
	14-144Z-4-2 interval 60-64 <sup>b</sup>	144 4 2W 60-64	215	1.21	–	570	6.5	0.97	1.45	0.707806	0.51188
	14-144Z-4-2 interval 143-146 <sup>b</sup>	144 4 2W 60-64	215	1.13	–	570	6.5	0.97	1.45	0.707806	0.51188
	14-144Z-4-3 interval 31-33 <sup>b</sup>	144 4 2W 60-64	215	0.74	–	570	6.5	0.97	1.45	0.707806	0.51188
	14-144Z-4-3 interval 100-103 <sup>b</sup>	144 4 2W 60-64	215	0.85	–	570	6.5	0.97	1.45	0.707806	0.51188
	14-144Z-5-1 interval 5-6 <sup>b</sup>	144 5 1W 123-125	265	0.39	–	446	22.5	4.2	6.39	0.708556	0.51211
	14-144Z-5-1 interval 143-143 <sup>b</sup>	144 5 1W 123-125	265	0.45	–	446	22.5	4.2	6.39	0.708556	0.51211
	14-144Z-7-1 interval 136-137 <sup>b</sup>	144 7 1W 80-82	299	0.28	–	270	28.8	5.4	8.42	0.710830	0.51211
	14-144Z-7-1 interval 123-124 <sup>b</sup>	144 7 1W 80-82	299	0.13	–	270	28.8	5.4	8.42	0.710830	0.51211
	14-144Z-8-3 interval 136-137 <sup>b</sup>	144 8 3W 130-135	328	0.29	–	349	29.4	5.5	8.19	0.710293	0.51210

<sup>a</sup> Data from from Van Soest (2000) (LAS1; LAG4), Davidson (1984;1986) (R8204; M8328; Altered basalt), Bezard et al. (2014; under review) (SL8344); Dufrane et al. (2009) (GUAD510) and Heat et al. (1998) (STV301; STV 324).

<sup>b</sup> Data indicated correspond to the samples analysed by Carpentier et al. (2008; 2009) named in the table.

**Table 3 : AFC model parameters**

<b>Endmember compositions<sup>a</sup></b>		
	<b>Initial Magma<sup>b</sup></b>	<b>Assimilant<sup>c</sup></b>
Sr (ppm)	296	790
Os (ppb)	0.36	0.02
La (ppm)	9.32	4.00
Sm (ppm)	2.60	1.84
Th (ppm)	2.41	0.50
<sup>87</sup> Sr/ <sup>86</sup> Sr	0.7051	0.7023
<sup>187</sup> Os/ <sup>188</sup> Os	0.1268	0.2450

<b>Bulk partition coefficients</b>		
	<b>Model 1</b>	<b>Model 2</b>
DSr	1.4	1.8
DOs	16	12
DTh	2.7	2.3
DLa	2	2.6
DSm	1.3	1.3
$r = Ma/Mc^c$	0.56	0.70

<sup>a</sup>used in both models 1 and 2

<sup>b</sup> composition of LAG 4 picrite

<sup>c</sup> determined iteratively